Correlations and fluctuations in a magnetized three-flavor PNJL model with and without inverse magnetic catalysis effect

Shijun Mao[*] and Shuai Yang

School of Physics, Xi'an Jiaotong University, Xi'an, Shaanxi 710049, China

(Received 29 April 2025; accepted 20 June 2025; published 15 July 2025)

The correlations $\chi_{11}^{BQ}, \chi_{11}^{BS}, \chi_{11}^{QS}$, and quadratic (quartic) fluctuations $\chi_{2,4}^{B}, \chi_{2,4}^{Q}, \chi_{2,4}^{S}$, of baryon number B, electric charge Q and strangeness S are investigated in a three-flavor PNJL model at finite temperature and magnetic field. The inverse magnetic catalysis (IMC) effect is introduced through the magnetic field dependent parameters $G(eB)$ or $T_0(eB)$, and we make comparison of the results in the cases with and without IMC effect. Since including IMC effect does not change the strength of phase transition under external magnetic field, it does not lead to qualitative difference in the correlations and fluctuations, but modifies their values. The correlations and fluctuations increase with temperature, and then show the peak around the pseudocritical temperatures of chiral restoration and deconfinement phase transitions. The peak structure in χ_{11}^{BQ}, χ_4^B, and χ_4^Q are much more apparent than in others. The correlations and fluctuations along the phase transition line under external magnetic field are characterized by the scaled correlations $\hat{\chi}_{11}^{XY} = \frac{\chi_{11}^{XY}(eB, T_{pc}^c(eB))}{\chi_{11}^{XY}(eB=0, T_{pc}^c(eB=0))}$ and scaled quadratic (quartic) fluctuations $\hat{\chi}_{2,4}^{X} = \frac{\chi_{2,4}^{X}(eB, T_{pc}^c(eB))}{\chi_{2,4}^{X}(eB=0, T_{pc}^c(eB=0))}$, with $X, Y = B, Q, S$, and $X \neq Y$ at the pseudocritical temperature T_{pc}^c of chiral restoration phase transition. They increase with magnetic fields due to the increase of phase transition strength under magnetic fields. Among them, $\hat{\chi}_{11}^{BQ}$ increases fastest, which may serve as the magnetometer of QCD.

DOI: 10.1103/fm5f-ctr3

I. INTRODUCTION

Motivated by the strong magnetic field in the core of compact stars and in the initial stage of relativistic heavy ion collisions, the study on quantum chromodynamics (QCD) phase structure under external electromagnetic fields has attracted much attention [1–56].

The lattice QCD (LQCD) simulations [7–15] observe the inverse magnetic catalysis (IMC) phenomena of u and d quarks, which means the decreasing chiral condensates near the pseudocritical temperature T_{pc}^c of chiral restoration phase transition and the decreasing pseudocritical temperature T_{pc}^c under external magnetic field. Meanwhile, it is reported that the renormalized Polyakov loop increases with magnetic fields and the transition temperature of deconfinement decreases as the magnetic field grows [7–12]. On analytical side, how to explain the inverse magnetic catalysis phenomena is the open question. Many scenarios are proposed [10,17–52], such as magnetic inhibition of mesons, sphalerons, gluon screening effect, weakening of strong coupling, and anomalous magnetic moment.

The thermodynamical properties of QCD matter are also influenced by the external magnetic field. Among the thermodynamic quantities, the correlations and fluctuations of the conserved charges are accessible in both theoretical calculations and experimental measurements. They can serve as the useful probes to study the QCD phase transitions, such as to identify the critical end point (CEP) of QCD phase diagram in the temperature-baryon chemical potential plane [57–63] and to serve as the possible magnetometer of QCD (probing the presence of magnetic fields in QCD matter) [15,64–67]. However, they are much less explored at the chiral restoration phase transition (crossover) with finite temperature, magnetic field and vanishing chemical potential. Except for the LQCD calculations [15,64–66], the analytical investigations at vanishing chemical potential, finite temperature and magnetic field [67–72] have been conducted in frame of the hadron resonance gas model, Polyakov loop extended Nambu-Jona-Lasinio (PNJL) model and Polyakov loop extended chiral quark model. It should be mentioned that with three-flavor quarks, the IMC effect is not well-considered [67–71].

In our current paper, the correlations $\chi_{11}^{BQ}, \chi_{11}^{BS}, \chi_{11}^{QS}$ and quadratic (quartic) fluctuations $\chi_{2,4}^{B}, \chi_{2,4}^{Q}, \chi_{2,4}^{S}$ of baryon number B, electric charge Q and strangeness S are studied in a three-flavor PNJL model at finite temperature and magnetic field. The IMC effect is introduced through the magnetic field dependent coupling between quarks $G(eB)$ [31,32,72–75] and magnetic field dependent interaction between quarks and Polyakov loop $T_0(eB)$ [43,46,52,72],

[*]Contact author: maoshijun@mail.xjtu.edu.cn

respectively. The comparison between the results in the cases with and without IMC effect are made. After the brief introduction, Sec. II presents our three-flavor magnetized PNJL model and the definition of correlations $\chi_{11}^{BQ}, \chi_{11}^{BS}, \chi_{11}^{QS}$, and quadratic (quartic) fluctuations $\chi_{2,4}^{B}, \chi_{2,4}^{Q}, \chi_{2,4}^{S}$. Section III discusses the numerical results of correlations and fluctuations at finite temperature and magnetic field in the cases without IMC effect and with IMC effect. Finally, we give the summary in Sec. IV.

II. THEORETICAL FRAMEWORK

The three-flavor PNJL model under external magnetic field is defined with the Lagrangian density [76–82],

$$
\begin{aligned}
\mathcal{L} &= \bar{\psi}(i\gamma^\mu D_\mu - \hat{m}_0)\,\psi + \mathcal{L}_4 + \mathcal{L}_6 - \mathcal{U}(\Phi,\bar{\Phi}),\\
\mathcal{L}_4 &= G\sum_{\alpha=0}^{8}[(\bar{\psi}\lambda_\alpha\psi)^2 + (\bar{\psi}i\gamma_5\lambda_\alpha\psi)^2],\\
\mathcal{L}_6 &= -K[\det\bar{\psi}(1+\gamma_5)\psi + \det\bar{\psi}(1-\gamma_5)\psi],\\
\mathcal{U}(\Phi,\bar{\Phi}) &= T^4\left[-\frac{b_2(t)}{2}\bar{\Phi}\Phi - \frac{b_3}{6}(\bar{\Phi}^3+\Phi^3) + \frac{b_4}{4}(\bar{\Phi}\Phi)^2\right].
\end{aligned} \tag{1}
$$

The covariant derivative $D^\mu = \partial^\mu + iQA^\mu - i\mathcal{A}^\mu$ couples quarks to the two external fields, the magnetic field $\mathbf{B} = \nabla\times\mathbf{A}$ and the temporal gluon field $\mathcal{A}^\mu = \delta_0^\mu \mathcal{A}^0$ with $\mathcal{A}^0 = g\mathcal{A}_a^0\lambda_a/2 = -i\mathcal{A}_4$ in Euclidean space. The gauge coupling g is combined with the SU(3) gauge field $\mathcal{A}_a^0(x)$ to define $\mathcal{A}^\mu(x)$, and λ_a are the Gell-Mann matrices in color space. We consider magnetic field $\mathbf{B} = (0,0,B)$ along the z-axis by setting $A_\mu = (0,0,xB,0)$ in Landau gauge, which couples quarks of electric charge $Q = \mathrm{diag}(Q_u, Q_d, Q_s) = \mathrm{diag}(2/3e, -1/3e, -1/3e)$. $\hat{m}_0 = \mathrm{diag}(m_0^u, m_0^d, m_0^s)$ is the current quark mass matrix in flavor space. The four-fermion interaction $\mathcal{L}_4$ represents the interaction in scalar and pseudoscalar channels, with Gell-Mann matrices $\lambda_\alpha, \alpha = 1, 2, \ldots, 8$ and $\lambda_0 = \sqrt{2/3}\mathbf{I}$ in flavor space. The six-fermion interaction or Kobayashi-Maskawa-'t Hooft term $\mathcal{L}_6$ is related to the $U_A(1)$ anomaly [83–87]. The Polyakov potential $\mathcal{U}(\Phi,\bar{\Phi})$ describes deconfinement, where Φ is the trace of the Polyakov loop $\Phi = (\mathrm{Tr}_c L)/N_c$, with $L(\mathbf{x}) = \mathcal{P}\exp[i\int_0^\beta d\tau\mathcal{A}_4(\mathbf{x},\tau)] = \exp[i\beta\mathcal{A}_4]$ and $\beta = 1/T$, the coefficient $b_2(t) = a_0 + a_1 t + a_2 t^2 + a_3 t^3$ with $t = T_0/T$ is temperature dependent, and the other coefficients b_3 and b_4 are constants.

It is useful to convert the six-fermion interaction into an effective four-fermion interaction in the mean field approximation, and the Lagrangian density can be rewritten as [88,89]

$$
\begin{aligned}
\mathcal{L} = {} & \bar{\psi}(i\gamma^\mu D_\mu - \hat{m}_0)\psi - \mathcal{U}(\Phi,\bar{\Phi}) + \sum_{a=0}^{8}[K_a^-(\bar{\psi}\lambda^a\psi)^2 + K_a^+(\bar{\psi}i\gamma_5\lambda^a\psi)^2] + K_{30}^-(\bar{\psi}\lambda^3\psi)(\bar{\psi}\lambda^0\psi) + K_{30}^+(\bar{\psi}i\gamma_5\lambda^3\psi)(\bar{\psi}i\gamma_5\lambda^0\psi)\\
& + K_{03}^-(\bar{\psi}\lambda^0\psi)(\bar{\psi}\lambda^3\psi) + K_{03}^+(\bar{\psi}i\gamma_5\lambda^0\psi)(\bar{\psi}i\gamma_5\lambda^3\psi) + K_{80}^-(\bar{\psi}\lambda^8\psi)(\bar{\psi}\lambda^0\psi) + K_{80}^+(\bar{\psi}i\gamma_5\lambda^8\psi)(\bar{\psi}i\gamma_5\lambda^0\psi) + K_{08}^-(\bar{\psi}\lambda^0\psi)(\bar{\psi}\lambda^8\psi)\\
& + K_{08}^+(\bar{\psi}i\gamma_5\lambda^0\psi)(\bar{\psi}i\gamma_5\lambda^8\psi) + K_{83}^-(\bar{\psi}\lambda^8\psi)(\bar{\psi}\lambda^3\psi) + K_{83}^+(\bar{\psi}i\gamma_5\lambda^8\psi)(\bar{\psi}i\gamma_5\lambda^3\psi) + K_{38}^-(\bar{\psi}\lambda^3\psi)(\bar{\psi}\lambda^8\psi)\\
& + K_{38}^+(\bar{\psi}i\gamma_5\lambda^3\psi)(\bar{\psi}i\gamma_5\lambda^8\psi),
\end{aligned} \tag{2}
$$

with the effective coupling constants,

$$
\begin{aligned}
K_0^\pm &= G \pm \frac{1}{3}K(\sigma_u + \sigma_d + \sigma_s),\\
K_1^\pm &= K_2^\pm = K_3^\pm = G \mp \frac{1}{2}K\sigma_s,\\
K_4^\pm &= K_5^\pm = G \mp \frac{1}{2}K\sigma_d,\\
K_6^\pm &= K_7^\pm = G \mp \frac{1}{2}K\sigma_u,\\
K_8^\pm &= G \mp \frac{1}{6}K(2\sigma_u + 2\sigma_d - \sigma_s),\\
K_{03}^\pm &= K_{30}^\pm = \mp\frac{1}{2\sqrt{6}}K(\sigma_u - \sigma_d),\\
K_{08}^\pm &= K_{80}^\pm = \mp\frac{\sqrt{2}}{12}K(\sigma_u + \sigma_d - 2\sigma_s),\\
K_{38}^\pm &= K_{83}^\pm = \pm\frac{1}{2\sqrt{3}}K(\sigma_u - \sigma_d),
\end{aligned} \tag{3}
$$

and chiral condensates,

$$
\sigma_u = \langle\bar{u}u\rangle, \qquad \sigma_d = \langle\bar{d}d\rangle, \qquad \sigma_s = \langle\bar{s}s\rangle. \tag{4}
$$

The thermodynamic potential in mean-field level contains the mean-field part and quark part,

$$
\begin{aligned}
\Omega &= 2G(\sigma_u^2 + \sigma_d^2 + \sigma_s^2) - 4K\sigma_u\sigma_d\sigma_s + \mathcal{U}(\Phi,\bar{\Phi}) + \Omega_q,\\
\Omega_q &= -\sum_{f=u,d,s}\frac{|Q_fB|}{2\pi}\sum_l \alpha_l\int\frac{dp_z}{2\pi}[3E_f\\
&\quad + T\ln(1 + 3\Phi e^{-\beta E_f^+} + 3\bar{\Phi}e^{-2\beta E_f^+} + e^{-3\beta E_f^+})\\
&\quad + T\ln(1 + 3\bar{\Phi}e^{-\beta E_f^-} + 3\Phi e^{-2\beta E_f^-} + e^{-3\beta E_f^-})],
\end{aligned}
$$

where $f = u, d, s$ means quark flavors, l Landau levels, $\alpha_l = 2 - \delta_{l0}$ spin factor and $E_f^\pm = E_f \pm \mu_f$ contains quark energy $E_f = \sqrt{p_z^2 + 2l|Q_fB| + m_f^2}$ of longitudinal momentum p_z and effective quark masses $m_u = m_0^u - 4G\sigma_u + 2K\sigma_d\sigma_s$, $m_d = m_0^d - 4G\sigma_d + 2K\sigma_u\sigma_s$, $m_s = m_0^s - 4G\sigma_s + 2K\sigma_u\sigma_d$, and quark chemical potential $\mu_u = \frac{\mu_B}{3} + \frac{2\mu_Q}{3}$, $\mu_d = \frac{\mu_B}{3} - \frac{\mu_Q}{3}$, $\mu_s = \frac{\mu_B}{3} - \frac{\mu_Q}{3} + \frac{\mu_S}{3}$, with μ_B, μ_Q, μ_S the chemical potential corresponding to the baryon number B, electric charge Q and strangeness S, respectively.

The ground state at finite temperature, chemical potential and magnetic field is determined by minimizing the thermodynamic potential,

$$\begin{aligned} &\frac{\partial\Omega}{\partial\sigma_f} = 0, \quad (f = u, d, s), \\ &\frac{\partial\Omega}{\partial\Phi} = 0, \\ &\frac{\partial\Omega}{\partial\bar{\Phi}} = 0. \end{aligned} \tag{5}$$

The thermodynamic potential Ω is a function of order parameters (chiral condensates σ_f and Polyakov loop $\Phi, \bar{\Phi}$), and hence we obtain five coupled gap equations.

At vanishing quark chemical potential ($\mu_B = \mu_Q = \mu_S = 0$) and finite temperature, the chiral symmetry restoration and deconfinement process are smooth crossover. By considering the derivative of the order parameters (chiral condensates and Polyakov loop) with respect to the temperature, the pseuocritical temperatures T_{pc}^c and T_{pc}^d of chiral restoration and deconfinement phase transitions are determined by the location of the peak of $\frac{d\sigma_{ud}}{dT}$ with $\sigma_{ud} = \frac{\sigma_u + \sigma_d}{2}$ and $\frac{d\Phi}{dT}$, respectively. The strength of chiral restoration and deconfinement phase transitions is characterized by the peak value of $\frac{d\sigma_{ud}}{dT}$ and $\frac{d\Phi}{dT}$, respectively.

The fluctuations and correlations of baryon number B, electric charge Q, and strangeness S can be obtained by taking the derivatives of the thermodynamic potential Ω with respect to the chemical potentials $\hat{\mu}_X = \mu_X/T$, $(X = B, Q, S)$, evaluated at zero quark chemical potential,

$$\chi_{i,j,k}^{B,Q,S} = -\frac{\partial^{i+j+k}(\Omega/T^4)}{\partial\hat{\mu}_B^i \partial\hat{\mu}_Q^j \partial\hat{\mu}_S^k}\bigg|_{\mu_X=0}. \tag{6}$$

In this work, we focus on the correlations $\chi_{11}^{BQ}, \chi_{11}^{BS}, \chi_{11}^{QS}$, quadratic fluctuations $\chi_2^B, \chi_2^Q, \chi_2^S$ and quartic fluctuations $\chi_4^B, \chi_4^Q, \chi_4^S$ at finite temperature, magnetic field and vanishing quark chemical potential. To understand the property of correlations and fluctuations along the phase transition line under external magnetic field, the scaled correlations $\hat{\chi}_{11}^{XY} = \frac{\chi_{11}^{XY}(eB, T_{pc}^c(eB))}{\chi_{11}^{XY}(eB=0, T_{pc}^c(eB=0))}$ and scaled quadratic (quartic) fluctuations $\hat{\chi}_{2,4}^X = \frac{\chi_{2,4}^X(eB, T_{pc}^c(eB))}{\chi_{2,4}^X(eB=0, T_{pc}^c(eB=0))}$, with $X, Y = B$, Q, S, and $X \neq Y$ at the pseudocritical temperature T_{pc}^c of chiral restoration phase transition are also studied.

III. NUMERICAL RESULTS

Because of the contact interaction in NJL model, the ultraviolet divergence cannot be eliminated through renormalization, and a proper regularization scheme is needed. In this part, we apply the covariant Pauli-Villars regularization [18]. By fitting the physical quantities, pion mass $m_\pi = 138$ MeV, pion decay constant $f_\pi = 93$ MeV, kaon mass $m_K = 495.7$ MeV, η' meson mass $m_{\eta'} = 957.5$ MeV in vacuum, we fix the current masses of light quarks $m_0^u = m_0^d = 5.5$ MeV, and obtain the parameters $m_0^s = 154.7$ MeV, $G\Lambda^2 = 3.627$, $K\Lambda^5 = 92.835$, $\Lambda = 1101$ MeV [89]. For the Polyakov potential, the parameters are chosen as [77] $a_0 = 6.75$, $a_1 = -1.95$, $a_2 = 2.625$, $a_3 = -7.44$, $b_3 = 0.75$, $b_4 = 7.5$, and $T_0 = 270$ MeV.

The typical results of PNJL model with the original parameters determined from the vacuum properties present the catalysis phenomena at finite temperature and vanishing quark chemical potential. The order parameters, chiral condensates $\sigma_u/\sigma_{u0}, \sigma_d/\sigma_{d0}, \sigma_s/\sigma_{s0}$ and Polyakov loop $\Phi, \bar{\Phi}$, increase with the magnetic field in the whole temperature region. The pseudocritical temperatures for chiral restoration and deconfinement phase transitions increase with the magnetic field. The strength of chiral restoration and deconfinement phase transitions also increases with the magnetic field (see the black line in Fig. 1 lower panel). It should be mentioned that the catalysis phenomena of chiral condensates at high temperature and pseudocritical temperature of chiral restoration phase transition under external magnetic field are contrary to LQCD results [7–15], but the increasing strength of chiral restoration phase transition with increasing magnetic field is consistent with LQCD results [7–9].

By fitting the LQCD reported decreasing pseudocritical temperature of chiral symmetry restoration $T_{pc}^c(eB)/T_{pc}^c(eB = 0)$ under external magnetic field [7], we introduce the IMC effect in our three-flavor PNJL model through a magnetic field dependent parameter $G(eB)$ and $T_0(eB)$, respectively, which represent the influence of external magnetic field to the quark-gluon interaction. On one side, the coupling between quarks plays a significant role in determining the spontaneous breaking and restoration of chiral symmetry. Considering the direct interaction between quarks and external magnetic field, a magnetic field dependent coupling $G(eB)$ [31,32,72–75] is introduced into the PNJL model. On the other side, the interaction between the Polyakov loop and sea quarks may be important for the mechanism of IMC [10]. A magnetic field dependent Polyakov loop scale parameter $T_0(eB)$ [43,46,52,72] is introduced into the PNJL model to mimic the reaction of the gluon sector to the presence of magnetic fields. As plotted in Fig. 1, $G(eB)$ and $T_0(eB)$ are both monotonic decreasing functions of magnetic field. We have checked that, with our fitted parameter $G(eB)$ or $T_0(eB)$, the increase (decrease) of chiral condensates with magnetic fields at the low (high) temperature, the increase of

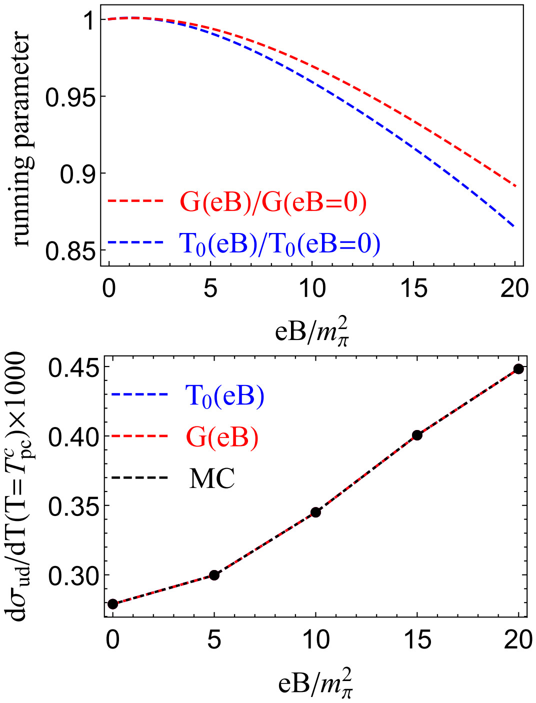

FIG. 1. (upper panel) Magnetic field dependent parameters $G(eB)$ (red line) and $T_0(eB)$ (blue line) fitted from LQCD reported decreasing pseudocritical temperature of chiral restoration phase transition $T^c_{pc}(eB)/T^c_{pc}(eB=0)$ under external magnetic field [7]. (lower panel) Strength of chiral restoration phase transition ($\frac{d\sigma_{ud}}{dT}$ at $T=T^c_{pc}$) under external magnetic field with IMC effect (blue and red lines) and without IMC effect (black line).

Polyakov loop with magnetic fields in the whole temperature region and the reduction of pseudocritical temperature of deconfinement phase transition under magnetic fields can be realized. Moreover, the inclusion of IMC effect does not change the strength of chiral restoration phase transition under external magnetic field, see Fig. 1 lower panel, where $\frac{d\sigma_{ud}}{dT}$ at the pseudocritical temperature of chiral restoration phase transition increases with magnetic fields and are almost coincident in the cases with and without IMC effect. This indicates that including IMC effect will not lead to qualitative difference in the results of correlations and fluctuations [70,72].

In the following part, we use the $G(eB)$ and $T_0(eB)$ scheme to consider the IMC effect, respectively, and make detailed comparison between the results of correlations and fluctuations with and without IMC effect.

Figure 2 depicts the correlations χ^{BQ}_{11}, $-\chi^{BS}_{11}$, χ^{QS}_{11} with IMC effect (blue and red lines) and without IMC effect (black lines) as functions of temperature T/T^c_{pc}, where T^c_{pc} is the pseudocritical temperature of chiral restoration phase transition with the given magnetic field when IMC effect is included or not. At fixed magnetic fields $eB/m_\pi^2 = 10$, 20, when considering the IMC effect with $G(eB)$ and $T_0(eB)$ schemes, the correlations χ^{BQ}_{11}, $-\chi^{BS}_{11}$, χ^{QS}_{11} increase with temperature and then have the peak structure. For χ^{BQ}_{11}, the peak is apparent and is located around the pseudocritical temperatures of chiral restoration and deconfinement phase transitions. $-\chi^{BS}_{11}$ and χ^{QS}_{11} have the wide peak. These properties are qualitatively similar as the case without IMC effect, but quantitative difference exists. The value of χ^{BQ}_{11} with IMC effect are larger than those without IMC effect around T^c_{pc} and in the higher temperature region. The value of $-\chi^{BS}_{11}$ and χ^{QS}_{11} including IMC effect with the $G(eB)$ ($T_0(eB)$) scheme are smaller (larger) than those without IMC effect around T^c_{pc}, but $-\chi^{BS}_{11}$ and χ^{QS}_{11} with IMC effect are larger than those without IMC effect in the higher-temperature region. In the right panels, we plot the scaled correlations $\hat{\chi}^{BQ}_{11}, \hat{\chi}^{BS}_{11}, \hat{\chi}^{QS}_{11}$ at the pseudocritical temperature of chiral restoration phase transition as functions of magnetic field with IMC effect (blue and red lines) and without IMC effect (black lines), and LQCD results [15,65,66] are depicted in the black vertical lines for references. $\hat{\chi}^{BQ}_{11}, \hat{\chi}^{BS}_{11}$, and $\hat{\chi}^{QS}_{11}$ increase with magnetic field. Different methods to consider IMC effect do not lead to qualitative difference in the results, and only cause some quantitative changes. Including the IMC effect with $G(eB)$ and $T_0(eB)$ schemes, $\hat{\chi}^{BQ}_{11}$ increases faster. $\hat{\chi}^{BS}_{11}$ and $\hat{\chi}^{QS}_{11}$ increase faster (slower) in the $T_0(eB)(G(eB))$ scheme.

Figure 3 plots the quadratic fluctuations $\chi^B_2, \chi^Q_2, \chi^S_2$ with IMC effect (blue and red lines) and without IMC effect (black lines) as functions of temperature T/T^c_{pc}, where T^c_{pc} is the pseudocritical temperature of chiral restoration phase transition with the given magnetic field when IMC effect is included or not. At fixed magnetic fields $eB/m_\pi^2 = 10$, 20, when considering the IMC effect with $G(eB)$ and $T_0(eB)$ schemes, $\chi^B_2, \chi^Q_2, \chi^S_2$ increase with temperature and have the wide peak around the pseudocritical temperatures of chiral restoration and deconfinement phase transitions. χ^B_2 and χ^Q_2 show more apparent peaks than χ^S_2. These properties are qualitatively similar as the case without IMC effect, but quantitative difference exists. For χ^B_2 and χ^Q_2, in case of weak magnetic field, their value including IMC effect with the $T_0(eB)$ ($G(eB)$) scheme is larger (smaller) than those without IMC effect around T^c_{pc}, and their value with IMC effect are larger than those without IMC effect in the higher-temperature region. In case of strong magnetic field, the value of χ^B_2 and χ^Q_2 with IMC effect are larger than those without IMC effect around T^c_{pc} and in the higher temperature region. For χ^S_2, in both weak and strong magnetic field cases, its value including IMC effect with the $T_0(eB)$ ($G(eB)$) scheme is larger (smaller) than those without IMC effect around T^c_{pc}, and the value with IMC effect are larger than those without IMC effect in the higher-temperature region. In the right panels, we plot the scaled quadratic fluctuations $\hat{\chi}^B_2, \hat{\chi}^Q_2, \hat{\chi}^S_2$ at the pseudocritical temperature of

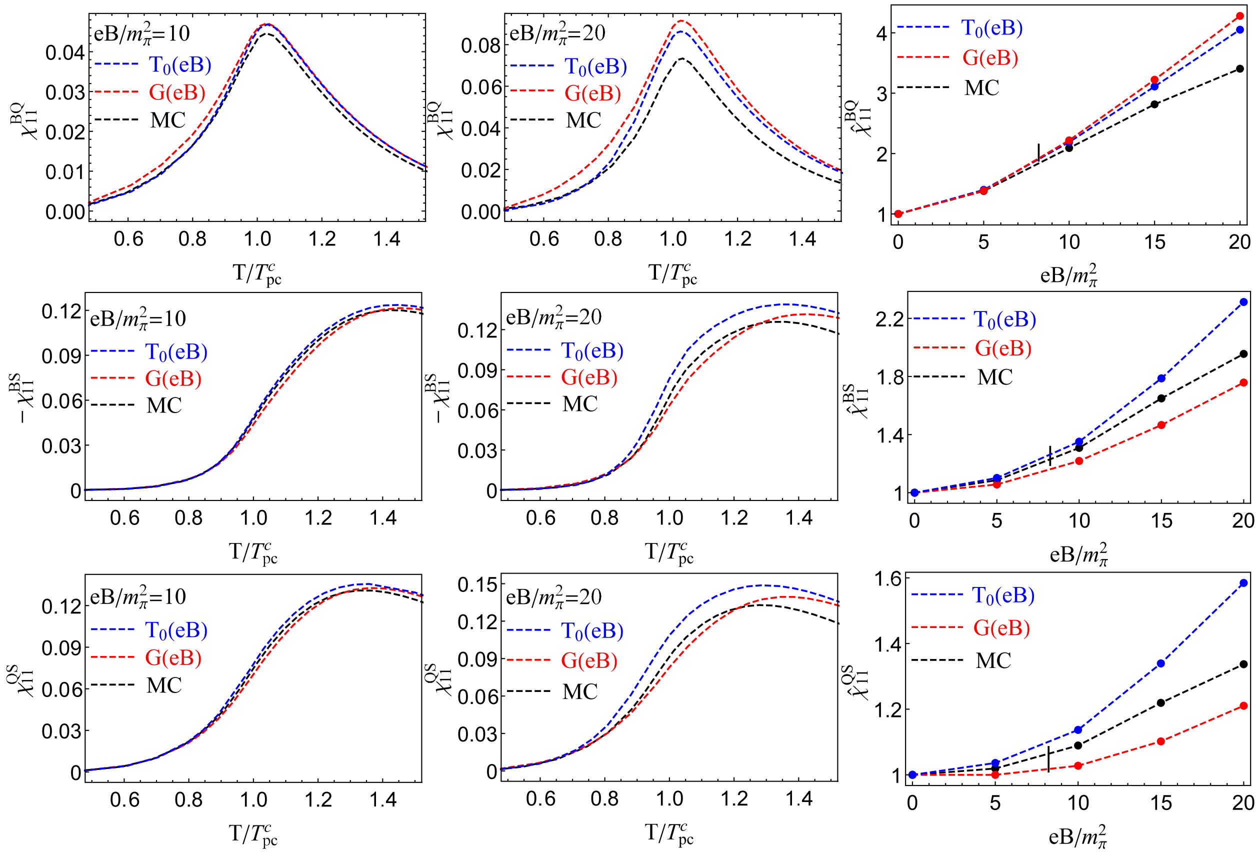

FIG. 2. (First row) The correlation χ_{11}^{BQ} as a function of temperature T/T_{pc}^c with fixed magnetic field $eB = 10m_\pi^2$ (left panel) and $eB = 20m_\pi^2$ (middle panel), and the scaled correlation $\hat{\chi}_{11}^{BQ}$ (right panel) at $T = T_{pc}^c$ as a function of magnetic field. (Second row) The correlation $-\chi_{11}^{BS}$ as a function of temperature T/T_{pc}^c with fixed magnetic field $eB = 10m_\pi^2$ (left panel) and $eB = 20m_\pi^2$ (middle panel), and the scaled correlation $\hat{\chi}_{11}^{BS}$ (right panel) at $T = T_{pc}^c$ as a function of magnetic field. (Third row) The correlation χ_{11}^{QS} as a function of temperature T/T_{pc}^c with fixed magnetic field $eB = 10m_\pi^2$ (left panel) and $eB = 20m_\pi^2$ (middle panel), and the scaled correlation $\hat{\chi}_{11}^{QS}$ (right panel) at $T = T_{pc}^c$ as a function of magnetic field. The black vertical lines in the right panels are the LQCD results [15,65,66]. For all panels, the blue (red) lines are the results in case of considering IMC effect in the $T_0(eB)$ ($G(eB)$) scheme, and the black lines are the results without IMC effect. T_{pc}^c is the pseudocritical temperature of chiral restoration phase transition with the given magnetic field when IMC effect is included or not.

chiral restoration phase transition as functions of magnetic field with IMC effect (blue and red lines) and without IMC effect (black lines), and LQCD results [15,65] are depicted in the black vertical lines for references. $\hat{\chi}_2^B$, $\hat{\chi}_2^Q$, and $\hat{\chi}_2^S$ increase with magnetic field. Different methods to consider IMC effect do not lead to qualitative difference in the results, and only cause some quantitative changes. In weak magnetic field cases, $\hat{\chi}_2^B$ and $\hat{\chi}_2^Q$ including the IMC effect with the $T_0(eB)$ ($G(eB)$) scheme increase faster (slower) than without IMC effect, and in strong magnetic field cases, $\hat{\chi}_2^B$ and $\hat{\chi}_2^Q$ with the IMC effect increase faster than without IMC effect. $\hat{\chi}_2^S$ increases faster in the $T_0(eB)$ scheme and increases slower in the $G(eB)$ scheme as magnetic field grows.

Figure 4 shows the quartic fluctuations χ_4^B, χ_4^Q, χ_4^S with IMC effect (blue and red lines) and without IMC effect (black lines) as functions of temperature T/T_{pc}^c, where T_{pc}^c is the pseudocritical temperature of chiral restoration phase transition with the given magnetic field when IMC effect is included or not. At fixed magnetic fields $eB/m_\pi^2 = 10$, 20, when considering the IMC effect with $G(eB)$ and $T_0(eB)$ schemes, χ_4^B, χ_4^Q, and χ_4^S increase with temperature and have the peak around the pseudocritical temperatures of chiral restoration and deconfinement phase transitions. χ_4^B and χ_4^Q show sharper peak than χ_4^S. These properties are qualitatively similar as the case without IMC effect, but quantitative difference exists. In the weak magnetic field case, quartic fluctuations χ_4^B, χ_4^Q, χ_4^S are not sensitive to the introduction of IMC effect. In the strong magnetic field case, the peak value of χ_4^B including IMC effect is larger than without IMC effect, the peak value of χ_4^Q including IMC effect with the $G(eB)$ ($T_0(eB)$) scheme is larger

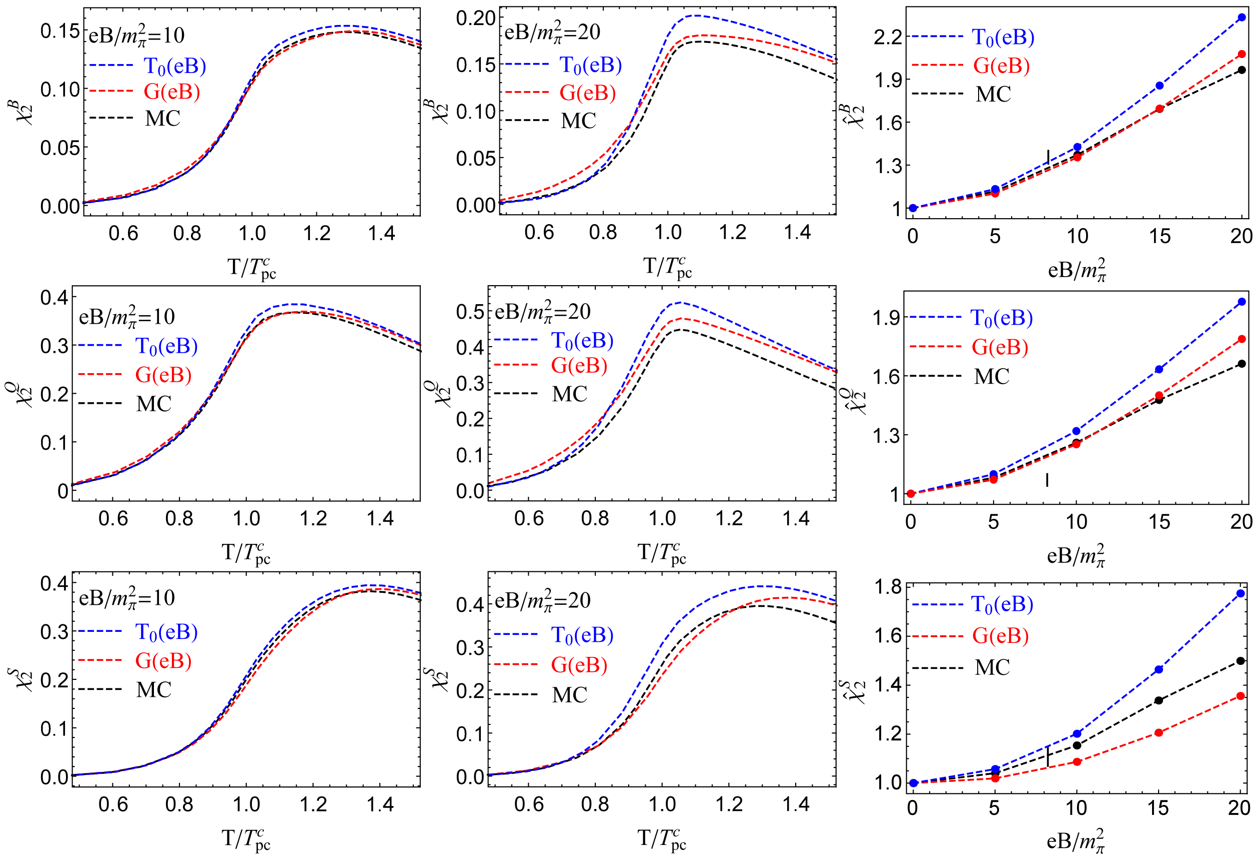

FIG. 3. (First row) The quadratic fluctuation χ_2^B as a function of temperature T/T_{pc}^c with fixed magnetic field $eB = 10m_\pi^2$ (left panel) and $eB = 20m_\pi^2$ (middle panel), and the scaled quadratic fluctuation $\hat{\chi}_2^B$ (right panel) at $T = T_{pc}^c$ as a function of magnetic field. (Second row) The quadratic fluctuation χ_2^Q as a function of temperature T/T_{pc}^c with fixed magnetic field $eB = 10m_\pi^2$ (left panel) and $eB = 20m_\pi^2$ (middle panel), and the scaled quadratic fluctuation $\hat{\chi}_2^Q$ (right panel) at $T = T_{pc}^c$ as a function of magnetic field. (Third row) The quadratic fluctuation χ_2^S as a function of temperature T/T_{pc}^c with fixed magnetic field $eB = 10m_\pi^2$ (left panel) and $eB = 20m_\pi^2$ (middle panel), and the scaled quadratic fluctuation $\hat{\chi}_2^S$ (right panel) at $T = T_{pc}^c$ as a function of magnetic field. The black vertical lines in the right panels are the LQCD results [15,65]. For all panels, the blue (red) lines are the results in case of considering IMC effect in the $T_0(eB)$ $(G(eB))$ scheme, and the black lines are the results without IMC effect. T_{pc}^c is the pseudocritical temperature of chiral restoration phase transition with the given magnetic field when IMC effect is included or not.

(smaller) than without IMC effect, and the value of χ_4^S with IMC effect is smaller (larger) than those without IMC effect around T_{pc}^c (in the higher-temperature region). In the right panels, we plot the scaled quartic fluctuations $\hat{\chi}_4^B, \hat{\chi}_4^Q, \hat{\chi}_4^S$ at the pseudocritical temperature of chiral restoration phase transition as functions of magnetic field with IMC effect (blue and red lines) and without IMC effect (black lines). They increase with magnetic field. Different methods to consider IMC effect do not lead to qualitative difference in the results, and only cause some quantitative changes. Including the IMC effect does not alter $\hat{\chi}_4^B$ too much. $\hat{\chi}_4^Q$ increases faster (slower) in the $G(eB)(T_0(eB))$ scheme. Including the IMC effect with $G(eB)$ and $T_0(eB)$ schemes, $\hat{\chi}_4^S$ increases slower than without IMC effect.

The peak structure of fluctuations and correlations is caused by the phase transition (crossover). When turning on the external magnetic field, the strength of phase transition increases (see Fig. 1 lower panel), and this leads to the enhancement of the fluctuations and correlations around the phase transition. It is noticeable that fluctuations and correlations related with strangeness $(\chi_2^S, \chi_4^S, -\chi_{11}^{BS}, \chi_{11}^{QS})$ are less sensitive to the magnetic field than others $(\chi_2^B, \chi_2^Q, \chi_4^B, \chi_4^Q, \chi_{11}^{BQ})$, and the peak structure of $\chi_2^S, \chi_4^S, -\chi_{11}^{BS}, \chi_{11}^{QS}$ is less apparent than $\chi_2^B, \chi_2^Q, \chi_4^B, \chi_4^Q, \chi_{11}^{BQ}$, either. The reason is that all up, down and strange quarks make contribution to $\chi_2^B, \chi_2^Q, \chi_4^B, \chi_4^Q, \chi_{11}^{BQ}$, but $\chi_2^S, \chi_4^S, -\chi_{11}^{BS}, \chi_{11}^{QS}$ are mainly related to strange quarks, which are much more heavier than up and down quarks. The quadratic fluctuations $\chi_2^B, \chi_2^Q, \chi_2^S$ and correlation $\chi_{11}^{BQ}, -\chi_{11}^{BS}, \chi_{11}^{QS}$ are qualitatively consistent with LQCD simulations [15,64]. The scaled correlations and fluctuations increase with magnetic field. Among them, $\hat{\chi}_{11}^{BQ}$ increases fastest, which may serve as a

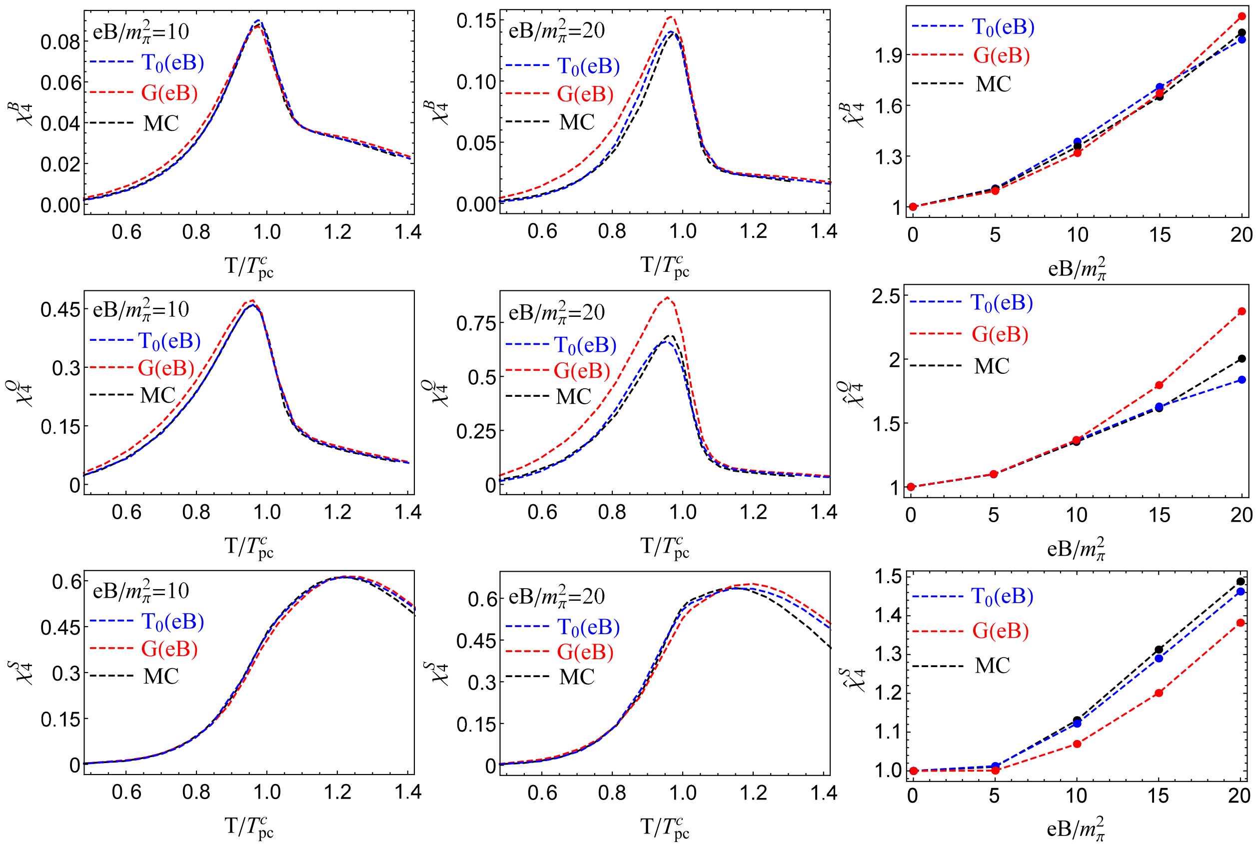

FIG. 4. (First row) The quartic fluctuation χ_4^B as a function of temperature T/T_{pc}^c with fixed magnetic field $eB = 10m_\pi^2$ (left panel) and $eB = 20m_\pi^2$ (middle panel), and the scaled quadratic fluctuation $\hat{\chi}_4^B$ (right panel) at $T = T_{pc}^c$ as a function of magnetic field. (Second row) The quartic fluctuation χ_4^Q as a function of temperature T/T_{pc}^c with fixed magnetic field $eB = 10m_\pi^2$ (left panel) and $eB = 20m_\pi^2$ (middle panel), and the scaled quadratic fluctuation $\hat{\chi}_4^Q$ (right panel) at $T = T_{pc}^c$ as a function of magnetic field. (Third row) The quartic fluctuation χ_4^S as a function of temperature T/T_{pc}^c with fixed magnetic field $eB = 10m_\pi^2$ (left panel) and $eB = 20m_\pi^2$ (middle panel), and the scaled quadratic fluctuation $\hat{\chi}_4^S$ (right panel) at $T = T_{pc}^c$ as a function of magnetic field. Here, the blue (red) lines are the results in case of considering IMC effect in the $T_0(eB)$ $(G(eB))$ scheme, and the black lines are the results without IMC effect. T_{pc}^c is the pseudocritical temperature of chiral restoration phase transition with the given magnetic field when IMC effect is included or not.

magnetometer of QCD [15,66]. These properties are qualitatively consistent with the LQCD results [15,65,66], depicted in the vertical lines in Figs. 2 and 3 right panels. At the quantitative level, $\hat{\chi}_{11}^{BQ}$, $\hat{\chi}_{11}^{BS}$, $\hat{\chi}_{11}^{QS}$, $\hat{\chi}_2^B$, and $\hat{\chi}_2^S$ are reasonably good, and $\hat{\chi}_2^Q$ overshoots the LQCD result.

IV. SUMMARY

The correlations $\chi_{11}^{BQ}, \chi_{11}^{BS}, \chi_{11}^{QS}$, and fluctuations $\chi_{2,4}^B$, $\chi_{2,4}^Q, \chi_{2,4}^S$ at finite temperature and magnetic field are investigated in frame of a three-flavor PNJL model. The IMC effect is introduced into the PNJL model by two methods, the magnetic field dependent coupling between quarks $G(eB)$, and magnetic field dependent interaction between quarks and Polyakov loop $T_0(eB)$. We make comparison of the results in the cases with and without IMC effect.

The PNJL model with IMC effect recovers the decreasing pseudocritical temperature of phase transitions under external magnetic field and the properties of order parameters reported in LQCD simulations. But the increasing strength of chiral restoration phase transition under external magnetic field is obtained in the cases with and without IMC effect. Therefore, the inclusion of IMC effect does not lead to qualitative difference in the results of correlations and fluctuations, and only causes some quantitative changes.

The correlations $\chi_{11}^{BQ}, \chi_{11}^{BS}, \chi_{11}^{QS}$, and fluctuations $\chi_{2,4}^B, \chi_{2,4}^Q, \chi_{2,4}^S$ show similar properties at finite temperature and magnetic field. The correlations and fluctuations first increase with temperature, and then show the peak around the pseudocritical temperatures of chiral restoration and deconfinement phase transitions. The peak structure in χ_{11}^{BQ}, χ_4^B, and χ_4^Q is much more apparent than in other correlations and fluctuations. To demonstrate the correlations and fluctuations along the phase transition line under external magnetic field, we calculate the scaled correlations $\hat{\chi}_{11}^{BQ}$, $\hat{\chi}_{11}^{BS}$, $\hat{\chi}_{11}^{QS}$, and scaled fluctuations $\hat{\chi}_{2,4}^{B}$, $\hat{\chi}_{2,4}^{Q}$, $\hat{\chi}_{2,4}^{S}$, at the pseudocritical temperature of chiral restoration phase transition. They increase with magnetic fields, which is caused by the increase of phase transition strength under external magnetic field. Among them, $\hat{\chi}_{11}^{BQ}$ increases fastest, which may serve as the magnetometer of QCD. These properties of correlations and quadratic fluctuations are qualitatively consistent with the LQCD results.

ACKNOWLEDGMENTS

The work is supported by the NSFC Grant No. 12275204.

DATA AVAILABILITY

The data are not publicly available. The data are available from the authors upon reasonable request.

[1] F. Preis, A. Rebhan, and A. Schmitt, Lect. Notes Phys. **871**, 51 (2013).
[2] R. Gatto and M. Ruggieri, Lect. Notes Phys. **871**, 87 (2013).
[3] V. A. Miransky and I. A. Shovkovy, Phys. Rep. **576**, 1 (2015).
[4] J. O. Anderson and W. R. Naylor, Rev. Mod. Phys. **88**, 025001 (2016).
[5] G. Q. Cao, Eur. Phys. J. A **57**, 264 (2021).
[6] M. D'Elia, Lect. Notes Phys. **871**, 181 (2013).
[7] G. S. Bali, F. Bruckmann, G. Endrödi, Z. Fodor, S. D. Katz, S. Krieg, A. Schaefer, and K. K. Szabo, J. High Energy Phys. 02 (2012) 044.
[8] G. S. Bali, F. Bruckmann, G. Endrödi, Z. Fodor, S. D. Katz, and A. Schaefer, Phys. Rev. D **86**, 071502 (2012).
[9] G. S. Bali, F. Bruckmann, G. Endrödi, Z. Fodor, S. D. Katz, and A. Schaefer, J. High Energy Phys. 08 (2014) 177.
[10] F. Bruckmann, G. Endrödiand T. G. Kovacs, J. High Energy Phys. 04 (2013) 112.
[11] V. G. Bornyakov, P. V. Buividovich, N. Cundy, O. A. Kochetkov, and A. Schaefer, Phys. Rev. D **90**, 034501 (2014).
[12] G. Endrödi, J. High Energy Phys. 07 (2015) 173.
[13] G. Endrödi, M. Giordano, S. D. Katz, T. G. Kovacs, and F. Pittler, J. High Energy Phys. 07 (2019) 007.
[14] H. T. Ding, S. T. Li, J. H. Liu, and X. D. Wang, Phys. Rev. D **105**, 034514 (2022).
[15] H. T. Ding, J. B. Gu, A. Kumar, and S. T. Li, arXiv:2503.18467.
[16] M. D'Elia, F. Manigrasso, F. Negro, and F. Sanfilippo, Phys. Rev. D **98**, 054509 (2018).
[17] K. Fukushima and Y. Hidaka, Phys. Rev. Lett. **110**, 031601 (2013).
[18] S. J. Mao, Phys. Lett. B **758**, 195 (2016).
[19] S. J. Mao, Phys. Rev. D **94**, 036007 (2016).
[20] S. J. Mao, Phys. Rev. D **97**, 011501(R) (2018).
[21] S. J. Mao, Chin. Phys. C **45**, 021004 (2021).
[22] S. J. Mao, Phys. Rev. D **106**, 034018 (2022).
[23] K. Kamikado and T. Kanazawa, J. High Energy Phys. 03 (2014) 009.
[24] J. Y. Chao, P. C. Chu, and M. Huang, Phys. Rev. D **88**, 054009 (2013).
[25] J. Braun, W. A. Mian, and S. Rechenberger, Phys. Lett. B **755**, 265 (2016).
[26] N. Mueller and J. M. Pawlowski, Phys. Rev. D **91**, 116010 (2015).
[27] T. Kojo and N. Su, Phys. Lett. B **720**, 192 (2013).
[28] A. Ayala, M. Loewe, A. J. Mizher, and R. Zamora, Phys. Rev. D **90**, 036001 (2014).
[29] A. Ayala, L. A. Hernandez, A. J. Mizher, J. C. Rojas, and C. Villavicencio, Phys. Rev. D **89**, 116017 (2014).
[30] A. Ayala, C. A. Dominguez, L. A. Hernandez, M. Loewe, and R. Zamora, Phys. Rev. D **92**, 096011 (2015).
[31] R. L. S. Farias, K. P. Gomes, G. Krein, and M. B. Pinto, Phys. Rev. C **90**, 025203 (2014).
[32] M. Ferreira, P. Costa, O. Lourenco, T. Frederico, and C. Providência, Phys. Rev. D **89**, 116011 (2014).
[33] F. Preis, A. Rebhan, and A. Schmitt, J. High Energy Phys. 03 (2011) 033.
[34] E. S. Fraga and A. J. Mizher, Phys. Rev. D **78**, 025016 (2008).
[35] E. S. Fraga and A. J. Mizher, Nucl. Phys. **A820**, 103C (2009).
[36] K. Fukushima, M. Ruggieri, and R. Gatto, Phys. Rev. D **81**, 114031 (2010).
[37] C. V. Johnson and A. Kundu, J. High Energy Phys. 12 (2008) 053.
[38] V. Skokov, Phys. Rev. D **85**, 034026 (2012).
[39] E. S. Fraga, J. Noronha, and L. F. Palhares, Phys. Rev. D **87**, 114014 (2013).
[40] R. Gatto and M. Ruggieri, Phys. Rev. D **82**, 054027 (2010).
[41] R. Gatto and M. Ruggieri, Phys. Rev. D **83**, 034016 (2011).
[42] M. Ferreira, P. Costa, and C. Providência, Phys. Rev. D **89**, 036006 (2014).
[43] M. Ferreira, P. Costa, D. P. Menezes, C. Providência, and N. N. Scoccola, Phys. Rev. D **89**, 016002 (2014).
[44] P. Costa, M. Ferreira, H. Hansen, D. P. Menezes, and C. Providência, Phys. Rev. D **89**, 056013 (2014).
[45] A. J. Mizher, M. N. Chernodub, and E. S. Fraga, Phys. Rev. D **82**, 105016 (2010).
[46] E. S. Fraga, B. W. Mintz, and J. Schaffner-Bielich, Phys. Lett. B **731**, 154 (2014).
[47] E. J. Ferrer, V.de la Incera, I. Portillo, and M. Quiroz, Phys. Rev. D **89**, 085034 (2014).
[48] E. J. Ferrer, V. de la Incera, and X. J. Wen, Phys. Rev. D **91**, 054006 (2015).
[49] J. Mei and S. J. Mao, Phys. Rev. D **102**, 114035 (2020).

[50] K. Xu, J. Y. Chao, and M. Huang, Phys. Rev. D **103**, 076015 (2021).
[51] J. Mei, R. Wen, S. J. Mao, M. Huang, and K. Xu, Phys. Rev. D **110**, 034024 (2024).
[52] S. J. Mao, Phys. Rev. D **110**, 054002 (2024).
[53] G. Cao and X. G. Huang, Phys. Rev. D **93**, 016007 (2016).
[54] W. R. Tavares, R. L. S. Farias, and S. S. Avancini, Phys. Rev. D **101**, 016017 (2020).
[55] W. R. Tavares, S. S. Avancini, and R. L. S. Farias, Phys. Rev. D **108**, 016017 (2023).
[56] G. Endrödiand G. Marko, Phys. Rev. D **109**, 034506 (2024).
[57] H. T. Ding, F. Karsch, and S. Mukherjee, Int. J. Mod. Phys. E **24**, 1530007 (2015).
[58] W. J. Fu, Commun. Theor. Phys. **74**, 097304 (2022).
[59] X. Luo and N. Xu, Nucl. Sci. Tech. **28**, 112 (2017).
[60] A. Pandav, D. Mallic, and B. Mohanty, Prog. Part. Nucl. Phys. **125**, 103960 (2022).
[61] A. Rustanmov, EPJ Web Conf. **276**, 01007 (2023).
[62] T. Nonaka, Acta Phys. Pol. B Proc. Suppl. **16**, 1 (2023).
[63] H. S. Ko (STAR Collaboration), Acta Phys. Pol. B Proc. Suppl. **16**, 1 (2023).
[64] H. T. Ding, S. T. Li, Q. Shi, and X. D. Wang, Eur. Phys. J. A **57**, 202 (2021).
[65] H. T. Ding, S. T. Li, J. H. Liu, and X. D. Wang, Acta Phys. Pol. B Proc. Suppl. **16**, 1 (2023).
[66] H. T. Ding, J. B. Gu, A. Kumar, S. T. Li, and J. H. Liu, Phys. Rev. Lett. **132**, 201903 (2024).
[67] K. Fukushima and Y. Hidaka, Phys. Rev. Lett. **117**, 102301 (2016).
[68] A. Bhattacharyya, S. K. Ghosh, R. Ray, and S. Samanta, Eur. Phys. Lett. **115**, 62003 (2016).
[69] G. Kadam, S. Pal, and A. Bhattacharyya, J. Phys. G **47**, 125106 (2020).
[70] W. J. Fu, Phys. Rev. D **88**, 014009 (2013).
[71] N. Chahal, S. Dutt, and A. Kumar, Phys. Rev. C **107**, 045203 (2023).
[72] S. J. Mao, Chin. Phys. C **49**, 063106 (2025).
[73] H. Liu, L. Yu, M. Chernodub, and M. Huang, Phys. Rev. D **94**, 113006 (2016).
[74] S. S. Avancini, M. Coppola, N. N. Scoccola, and J. C. Sodré, Phys. Rev. D **104**, 094040 (2021).
[75] S. J. Mao and Y. M. Tian, Phys. Rev. D **106**, 094017 (2022).
[76] P. N. Meisinger and M. C. Ogilvie, Phys. Lett. B **379**, 163 (1996).
[77] P. N. Meisinger, T. R. Miller, and M. C. Ogilvie, Phys. Rev. D **65**, 034009 (2002).
[78] K. Fukushima, Phys. Lett. B **591**, 277 (2004).
[79] A. Mocsy, F. Sannino, and K. Tuominen, Phys. Rev. Lett. **92**, 182302 (2004).
[80] E. Megias, E. Ruiz Arriola, and L. L. Salcedo, Phys. Rev. D **74**, 065005 (2006).
[81] C. Ratti, M. A. Thaler, and W. Weise, Phys. Rev. D **73**, 014019 (2006).
[82] S. K. Ghosh, T. K. Mukherjee, M. G. Mustafa, and R. Ray, Phys. Rev. D **73**, 114007 (2006).
[83] T. Kunihiro and T. Hatsuda, Phys. Lett. B **206**, 385 (1988).
[84] V. Bernard, R. L. Jaffe, and U. G. Meissner, Nucl. Phys. **B308**, 753 (1988).
[85] H. Reinhardt and R. Alkofer, Phys. Lett. B **207**, 482 (1988).
[86] G.'t Hooft, Phys. Rev. D **14**, 3432 (1976).
[87] G.'t Hooft, Phys. Rep. **142**, 357 (1986).
[88] P. Rehberg, S. P. Klevansky, and J. Huefner, Phys. Rev. C **53**, 410 (1996).
[89] J. Mei, T. Xia, and S. J. Mao, Phys. Rev. D **107**, 074018 (2023); **110**, 119901(E) (2024).